Effects of Surface Anchoring Groups (Carboxylate vs Phosphonate) in Ruthenium-Complex-Sensitized TiO_2 on Visible Light Reactivity in Aqueous Suspensions

Eunyoung Bae,[†] Wonyong Choi,*[,†,‡] Jaiwook Park,[‡] Hyeon Suk Shin,[‡] Seung Bin Kim,[‡] and Jae Sung Lee[†,§]

School of Environmental Science and Engineering, Department of Chemistry, and Department of Chemical Engineering, Pohang University of Science and Technology, Pohang 790-784, Korea

Received: May 23, 2004; In Final Form: June 24, 2004

This study compares the visible light reactivities and properties of two sensitized Pt/TiO_2 photocatalysts ($Pt/TiO_2/RuL_3$) on which ruthenium bipyridyl complexes (RuL_3) are anchored through carboxylic (c-RuL_3) or phosphonic (p-RuL_3) acid groups. The photoreductive dechlorination of CCl_4 and trichloroacetate (TCA) and the hydrogen production in aqueous suspensions were used as probe reactions for the visible light reactivity. The molar absorptivity of p-RuL_3 was lower than that of c-RuL_3, but Pt/TiO_2/p-RuL_3 exhibited higher visible light activities than Pt/TiO_2/c-RuL_3 for all tested reactions. On the other hand, the steady-state photocurrent obtained with the Pt/TiO_2/p-RuL_3 (or TiO_2/p-RuL_3) electrode was lower than that obtained with the Pt/TiO_2/c-RuL_3 (or TiO_2/c-RuL_3) electrode. As for the sensitizer adsorption, more p-RuL_3 than c-RuL_3 adsorbed on a TiO_2 surface over a wide pH range: the adsorption of p-RuL_3 decreased above pH 7, whereas that of c-RuL_3 was reduced even at pH >4. Therefore, the photoreactivity of Pt/TiO_2/p-RuL_3 was higher than that of Pt/TiO_2/c-RuL_3 in the whole pH region tested. However, both sensitizer systems were not stable in aqueous solutions not only under visible light illumination but also in the dark. Both Pt/TiO_2/c-RuL_3 and Pt/TiO_2/p-RuL_3 in water gradually lost their photoreactivities with time, although the reactivity of the latter was consistently higher than that of the former. Ruthenium complexes on TiO_2 were slowly photodegraded under visible light, and both carboxylate and phosphonate linkages anchored on the TiO_2 surface were hydrolyzed in the absence of light, which was supported by FT-IR analysis.

Introduction

Semiconductor photocatalysts use photoenergy to drive many kinds of redox chemical reactions such as water splitting,[1−3] CO_2 conversion,[4−6] and pollutant degradation.[7] In particular, TiO_2 photocatalysts have demonstrated successful performances in degrading a wide variety of organic compounds in water and air under UV illumination.[7−9] However, the lack of visible light activity hinders their practical applications. Utilization of visible light in destroying recalcitrant pollutants is an essential basis to developing solar remediation technologies. Various methods have been attempted to make TiO_2 photocatalysts utilize visible light, which include impurity doping[10,11] and dye sensitization.[12−18]

Dye sensitization of TiO_2 has been extensively studied for solar cells in which dye molecules attached on the TiO_2 surface are excited by absorbing visible light and subsequently inject electrons into the conduction band (CB) of TiO_2 to generate photocurrent through an external circuit.[12−15] If the injected CB electrons are transferred to reducible substrates on the surface instead of being directed to the external circuit, a photoreductive conversion can be achieved under visible light. This approach is a basis of developing sensitized visible light photocatalysts. Some of the most successful sensitizers being used are derivatives of ruthenium bipyridyl complexes, which have been extensively studied for dye-sensitized solar cells but much less investigated for visible light photocatalysts. This group has previously demonstrated that TiO_2 particles sensitized by the ruthenium complexes successfully degraded perchloro compounds (e.g., CCl_4 and trichloroacetate (TCA)) in water under visible light and that the codeposition of Pt nanoparticles on TiO_2 along with the ruthenium sensitizer dramatically increased the visible light reactivity.[17,18] The key elementary steps in this sensitized process are illustrated in Scheme 1. On the other hand, the ruthenium complexes that were bonded to the TiO_2 surface via a carboxylate linkage were not stable in water and gradually lost their activity with time. The hydrolysis of the carboxylate linkage seems to inhibit the efficient electron transfer from the

SCHEME 1: Visible Light-Induced Reduction (e.g., Dechlorination, H_2 Production) on $Pt/TiO_2/RuL_3$ Particles in Water[a]

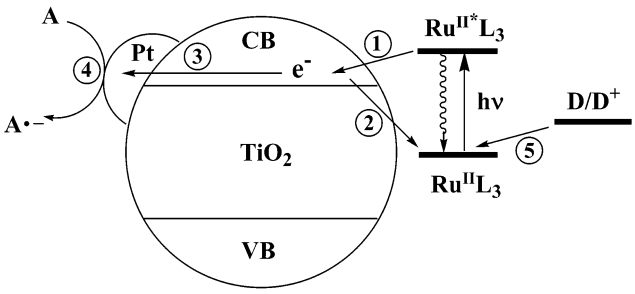

[a] The numbers represent the major electron pathways: (1) electron injection from the excited sensitizer to CB; (2) back electron transfer to the oxidized sensitizer ($Ru^{III}L_3$); (3) electron migration and trapping in Pt deposits; (4) interfacial electron transfer to a substrate or electron acceptor (A) (e.g., CCl_4, TCA) on Pt; (5) sensitizer regeneration by an electron donor (D) (H_2O in this case).

* To whom correspondence should be addressed. E-mail: wchoi@postech.ac.kr.
† School of Environmental Science and Engineering.
‡ Department of Chemistry.
§ Department of Chemical Engineering.

10.1021/jp047777p CCC: $27.50
Published on Web 08/24/2004

chromophoric ruthenium center to TiO_2 CB. A stronger linkage is needed in order to develop practical and durable Ru-sensitized TiO_2 photocatalysts (RuL_3/TiO_2).

This study compares the visible light reactivities and characteristics of two RuL_3/TiO_2 systems in which the ruthenium bipyridyl complexes are anchored to a TiO_2 surface through carboxylic ($-COOH$) and phosphonic acid ($-PO_3H_2$) groups, respectively. The phosphonate linkage to a TiO_2 surface has been suggested to be stronger and more stable than the carboxylate linkage in organic solvents.[19−24] However, no information about the visible light reactivity and stability in an aqueous system is available. The visible light reactivities of the two linkage systems in water were measured for both the photoreductive dechlorination of CCl_4 and TCA and the H_2 production with varying several experimental parameters.

Experimental Section

Sensitizer Preparation and Characterization. $Ru^{II}(4,4'\text{-}(CO_2H)_2bpy)_3$ and $Ru^{II}(bpy)_2(4,4'\text{-}(PO_3H_2)_2bpy)$ complexes (bpy is 2,2′-bipyridine) were synthesized and used as a sensitizer of TiO_2. Throughout this paper, the former and latter sensitizers will be referred to as **c-RuL$_3$** and **p-RuL$_3$**, respectively.

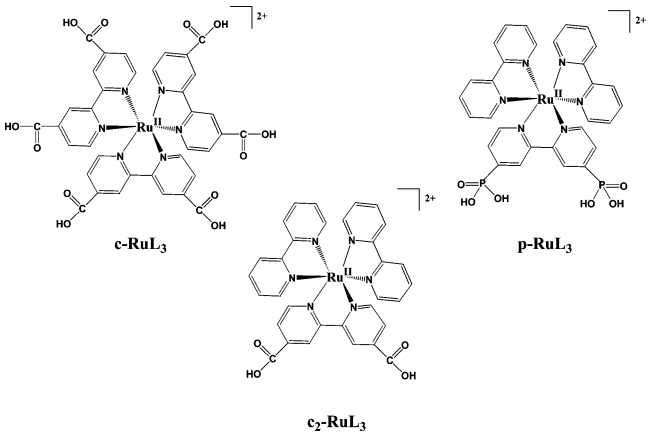

As for the Ru complex with the carboxylate group, we originally intended to use $Ru^{II}(bpy)_2(4,4'\text{-}(CO_2H)_2bpy)$ (abbreviated as **c$_2$-RuL$_3$**) instead of $Ru^{II}(4,4'\text{-}(CO_2H)_2bpy)_3$ (**c-RuL$_3$**). The two complexes differ in the number of binding groups (2 vs 6). Since p-RuL_3 has only two binding groups, using c_2-RuL_3, which has the same number of binding groups as p-RuL_3, is logical. However, c_2-RuL_3 hardly adsorbed on a TiO_2 surface in water (see Figure 4) and hence cannot be used in this study. The effects of anchoring groups (carboxylate vs phosphonate) on the photoreactivity should be compared on the basis of the same surface concentration of ruthenium sensitizers, and the concentrations of c-RuL_3 and p-RuL_3 adsorbed on the TiO_2 surface were the same at pH 3 (see Figure 4).

c-RuL_3[16] and p-RuL_3[22] were prepared by following literature methods. c-RuL_3 was available from our previous studies.[17,18] c_2-RuL_3 was synthesized through reacting *cis*-$Ru(bpy)_2Cl_2$ with 4,4′-dicarboxy-2,2′-bipyridine. p-RuL_3 was synthesized through a seven-step route: starting from 2,2′-bipyridine through 2,2′-bipyridyl-*N*,*N*′-dioxide,[25] 4,4′-dinitro-2,2′-bipyridine-1,1′-dioxide,[26] 4,4′-dibromo-2,2′-bipyridine-1,1′-dioxide,[27] 4,4′-dibromo-2,2′-bipyridine,[27] 4,4′-diethyl phosphonato-2,2′-bipyridine,[28] $\{Ru(bpy)_2[(4,4'\text{-}PO_3Et_2)_2bpy]\}(PF_6)_2$,[21] and finally to $\{Ru(bpy)_2[(4,4'\text{-}PO_3H_2)_2bpy]\}Br_2$.[22] The synthesized ruthenium complex sample was carefully purified by removing free bipyridyl ligands through precipitation and recrystallization. The counteranions of c-RuL_3 and p-RuL_3 were chlorides and bromides, respectively. Since c-RuL_3 was not readily dissolved at acidic pH, its stock solution of 100 μM was prepared at pH 11. The stock solution of 100 μM p-RuL_3 was at pH 4.

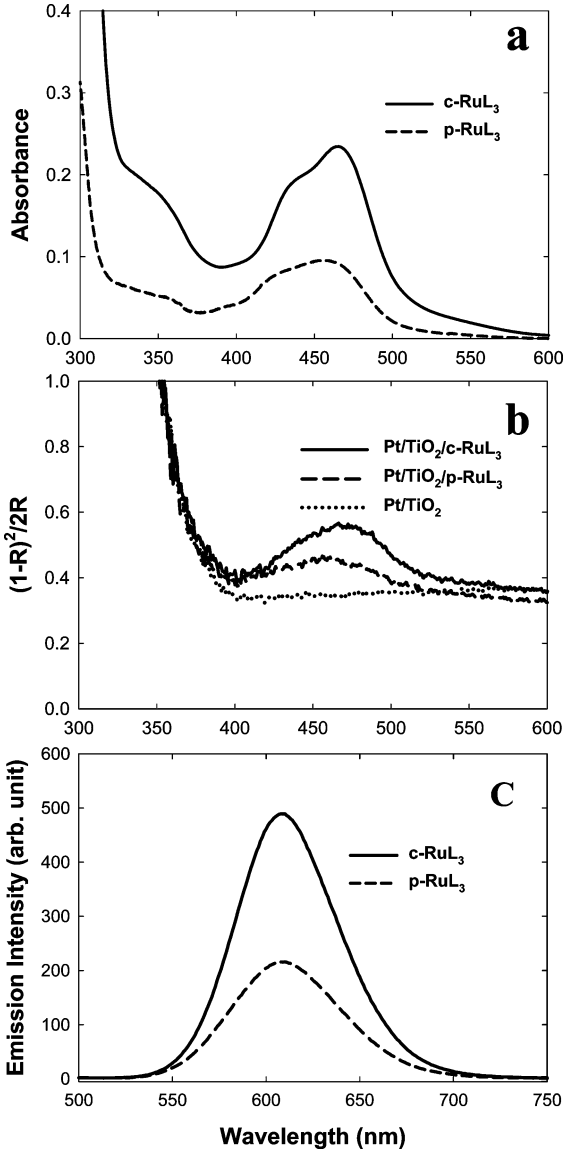

Figure 1. (a) UV−vis absorption spectra of 10 μM c-RuL_3 (pH 11) and p-RuL_3 (pH 4) in aqueous solution. (b) UV−vis diffuse-reflectance (expressed in Kubelka−Munk units, R = reflectance) spectra of Pt/TiO_2, Pt/TiO_2/c-RuL_3, and Pt/TiO_2/p-RuL_3 powders that were diluted in barium sulfate (50 wt % of sample). (c) Fluorescence emission spectra of 10 μM c-RuL_3 (pH 11) and p-RuL_3 (pH 4) in aqueous solution (λ_{ex} = 460 nm).

Figure 1a compares the UV−vis absorption spectra of the c-RuL_3 and p-RuL_3 complexes in water (10 μM). The absorption spectra of these complexes were typical of the ruthenium polypyridyl complexes with an intense UV band (~300 nm) assigned to ligand-centered $\pi \rightarrow \pi^*$ transitions and a broad band in the visible region due to metal-to-ligand charge-transfer (MLCT) transitions ($d \rightarrow \pi^*$).[22] The maximum of the MLCT band is located at λ_{max} = 465 nm for c-RuL_3 at pH 11 and λ_{max} = 456 nm for p-RuL_3 at pH 4. The molar absorptivities of c-RuL_3 and p-RuL_3 were determined to be 2.3×10^4 and 9.5×10^3 M^{-1} cm^{-1}, respectively, and were used in determining the concentration of the sensitizer. In accordance with our evaluation, the molar absorptivities of c-RuL_3 and p-RuL_3 have been reported to be 2.1×10^4 M^{-1} cm^{-1} (at λ_{max} = 467 nm) in water[29] and 9.3×10^3 M^{-1} cm^{-1} (at λ_{max} = 458 nm) in

methanol,[22] respectively. The fluorescence emission spectra of c-RuL_3 and p-RuL_3 in water were obtained with a spectrofluorometer (Shimadzu RF-5301) and compared in Figure 1c. The MLCT emission (λ_{ex} = 460 nm) maxima of both sensitizers are at 608 nm.

Chemicals. TiO_2 (Degussa P25), a mixture of 80% anatase and 20% rutile with an average surface area of 50 ± 15 m^2/g, was used as a photocatalyst. CCl_4 (J. T. Baker) was purified by distillation. Trichloroacetate (TCA, Fluka), chloroplatinic acid ($H_2PtCl_6 \cdot 6H_2O$) (Aldrich), 2-propanol (Fluka), and ethylenediaminetetraacetic acid (EDTA, Aldrich) were used as received. Deionized water used was ultrapure (18 MΩ cm) and was prepared by a Barnstead purification system.

Photocatalyst Preparation and Characterization. Platinum nanoparticles were loaded onto TiO_2 particles using a photodeposition method. The platinization was carried out in an aqueous suspension of TiO_2 (0.5 g/L) in the presence of 1 M methanol (electron donor) and 1×10^{-4} M chloroplatinic acid (H_2PtCl_6) under UV irradiation for 30 min (with a 200 W mercury lamp). After irradiation, the Pt/TiO_2 powder was filtered and washed with distilled water. A typical Pt loading on TiO_2 was estimated to be ca. 3 wt %. Transmission electron microscopic images of Pt/TiO_2 showed Pt particles with a size range of 1−4 nm dispersed on TiO_2 particles (20−30 nm diameter).

The Pt/TiO_2 powder was redispersed in distilled water (0.5 g/L) under sonication, and then the ruthenium sensitizer was added. The typical sensitizer concentration added to the suspension was 10 μM. No electron donor to regenerate the oxidized sensitizer was added in the suspension. The adsorption of the sensitizer on TiO_2 was measured as a function of pH, and the amount of the sensitizer adsorbed on TiO_2 was calculated from the absorbance difference (ΔA) between the initial sensitizer solution and the filtered solution of sensitizer-added suspension. At pH 3, all sensitizer molecules quantitatively adsorbed on TiO_2: the UV−vis absorption and emission spectra showed no sign of sensitizers present in the filtrate (through a 0.45 μm PTFE filter) of the equilibrated sensitizer-added TiO_2 suspension. Therefore, all experiments in this work were carried out at pH 3. When the heat-treated samples were used, Pt/TiO_2 (0.015 g), p-RuL_3 (1.7×10^{-4} g), and water (20 mL) at pH 3 were placed in a Teflon-lined steel autoclave. The sealed autoclave was heated at 120 °C in an oven for 3 h. After the hydrothermal treatment, the Pt/TiO_2/p-RuL_3 powder was filtered, washed with distilled water, and dried under air. Adsorbed sensitizers could be quantitatively desorbed from TiO_2 surface at pH 11, and their concentration was compared before and after the photoreaction.

The UV−vis absorption spectra of the sensitized TiO_2 powders were recorded with a UV−vis spectrophotometer (Shimadzu UV-2401PC) equipped with a diffuse-reflectance attachment (Shimadzu ISR-2200). Figure 1b compares the UV−vis diffuse reflectance spectra of Pt/TiO_2, Pt/TiO_2/c-RuL_3, and Pt/TiO_2/p-RuL_3 powders that were diluted in $BaSO_4$ powder with a 1:1 weight ratio. The characteristic MLCT transition band of RuL_3 sensitizers on TiO_2 was observed at the same position as in their solution spectra (Figure 1a). c-RuL_3 has higher absorption than p-RuL_3 in the visible region, both as a free molecule and as a surface complex.

FTIR spectra of TiO_2/RuL_3 powder samples were recorded with a resolution of 4 cm^{-1} using a Bomem DA8 FTIR spectrometer equipped with a liquid nitrogen cooled MCT detector. A Praying Mantis attachment from Harrick Scientific Corp. was used for the diffuse-reflectance infrared Fourier transform spectroscopic (DRIFTS) measurements. To ensure a high signal-to-noise ratio, 512 interferograms were added for each measurement. Both sample and source compartments were evacuated. DRIFT spectra of the free c-RuL_3 and TiO_2/c-RuL_3 were obtained using powder samples diluted in KBr powder and were referenced against KBr. On the other hand, DRIFT spectra of TiO_2/p-RuL_3 were obtained using the pure sample powder and were referenced against TiO_2 (IR absorption expressed in Kubelka−Munk function) to eliminate the strong IR absorption background from TiO_2 below 1000 cm^{-1}. The IR spectrum of free p-RuL_3 was obtained in a transmission mode using a p-RuL_3 sample cast on a ZnSe window. The samples were vacuum-dried at 35 °C for 24 h before the DRIFTS analysis.

Photoreactivity Measurements. The visible light reactivities of Pt/TiO_2/c-RuL_3 and Pt/TiO_2/p-RuL_3 were tested for both photoreductive dechlorination of CCl_4 and TCA and H_2 production. The light source for photolysis was a 300 W (or 450 W for H_2 production) Xe-arc lamp (Oriel). Light passed through a 10 cm IR water filter and a UV cutoff filter (λ >420 nm) and then was focused onto a 30 mL reactor. Since O_2 molecules compete for CB electrons with the reducible substrates, dissolved O_2 was removed by N_2 sparging before irradiation. The saturated stock solution of CCl_4 (5 mM) was prepared by stirring excess CCl_4 in deoxygenated distilled water, and a desired concentration (usually 1 mM) of CCl_4 was made by dilution. The reactor was sealed from the ambient air during the photolysis. The TCA concentration used was typically 1 mM and was prepared by the dilution of an aqueous stock solution (10 mM). The photoirradiation of a TCA-containing suspension was carried out under continuous N_2 sparging, because TCA is nonvolatile. Sample aliquots of 1 mL were collected from the reactor intermittently during the irradiation and analyzed for chlorides with an ion chromatograph (IC). The IC system was a Dionex DX-120 equipped with a Dionex IonPac AS14 (4 mm × 250 mm) column and a conductivity detector. As for the H_2 production experiments, the aqueous solution containing Pt/TiO_2/RuL_3 and EDTA (10 mM) at pH =3 was deaerated by N_2 sparging before irradiation. The amount of H_2 production was analyzed using a HP6890A GC equipped with a TCD detector and a molecular sieve 5A column. Light intensity was measured by chemical actinometry using (*E*)-α-(2,5-dimethyl-3-furylethylidene)(isopropylidene)succinic anhydride (Aberchrome 540),[31] as described elsewhere.[17] A typical incident light intensity was measured to be about 4.7×10^{-3} einstein L^{-1} min^{-1} in the wavelength range 420−550 nm.

Photoelectrochemical Measurements. The photoelectrochemical characteristics of the RuL_3/TiO_2 and RuL_3/Pt/TiO_2 electrodes were compared. TiO_2 electrodes were prepared as described previously.[30] A 0.5 mL portion of a TiO_2 suspension (5 wt %) was spread over an indium tin oxide (ITO) glass plate (3 × 3 cm^2; Samsung), and then the excess suspension was removed from the plate. This TiO_2/ITO electrode was dried in air for 30 min and heated at 450 °C for 30 min. For Pt deposition onto the TiO_2/ITO electrode, the electrode was immersed in an aqueous solution of 1×10^{-4} M H_2PtCl_6 and 1 M methanol and illuminated with a 200 W Hg lamp for 30 min. For sensitization of the TiO_2 and Pt/TiO_2 electrode, the electrode was immersed in an aqueous solution of RuL_3 (10 μM, pH 3.0) for 24 h. The resulting sensitized TiO_2 and Pt/TiO_2 electrodes were washed with distilled water (pH 3.0) and dried at room temperature for 30 min. The preparation of the Pt/TiO_2/p-RuL_3 electrode underwent an additional heat-treatment step (120 °C, 3 h). The photoelectrochemical cell was cylindrical and had a

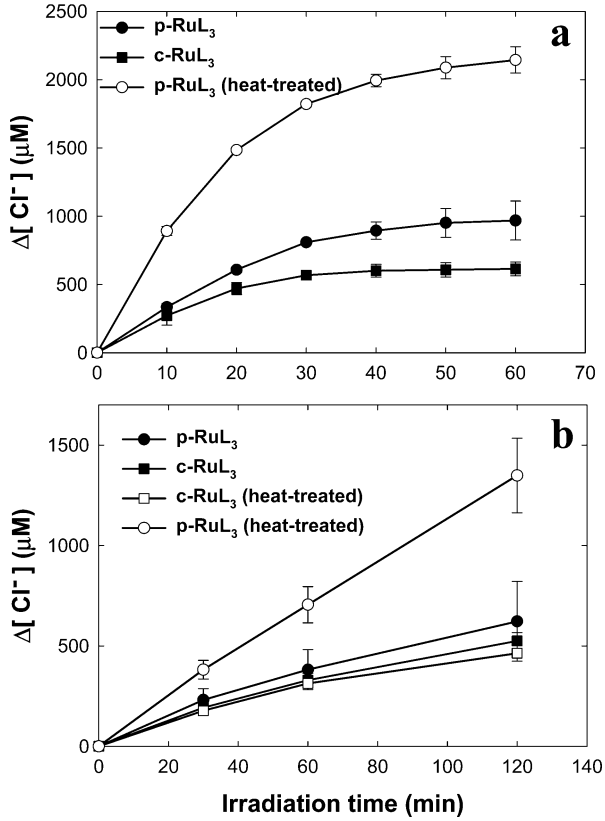

Figure 2. Time profiles of chloride production from (a) CCl_4 and (b) TCA degradation on $Pt/TiO_2/c\text{-}RuL_3$ and $Pt/TiO_2/p\text{-}RuL_3$ under visible light. Two different $Pt/TiO_2/p\text{-}RuL_3$ samples (one that was heat-treated in an autoclave and one without the heat treatment) were compared. The experimental conditions were as follows: $[TiO_2] = 0.5$ g/L, $pH_i = 3$, $[RuL_3]_i = 10\ \mu M$, $[CCl_4] = [TCA] = 1$ mM, $\lambda > 420$ nm, and initially N_2-saturated for CCl_4 or continuously N_2-sparged for the TCA case.

working electrode (RuL_3/TiO_2 or $RuL_3/Pt/TiO_2$), a reference saturated calomel electrode (SCE), and a counter graphite rod. The electrolyte used was 10 mM NaCl or 10 mM NaCl + 1 mM TCA at pH 3. The photoelectrochemical response was measured by a potentiostat (EG&G, Model 263A) that was connected to a computer.

Results and Discussion

Visible-Light-Sensitized Dechlorination on $Pt/TiO_2/c\text{-}RuL_3$ vs $Pt/TiO_2/p\text{-}RuL_3$. Figure 2 compares the visible-light-induced dechlorination from CCl_4 (Figure 2a) and TCA (Figure 2b) degradation on $Pt/TiO_2/c\text{-}RuL_3$ and $Pt/TiO_2/p\text{-}RuL_3$. The excited sensitizer injects electrons to TiO_2 CB, and the subsequent dechlorination is initiated by transferring CB electrons to CCl_4 or TCA (reactions 1−3).[18] The reported excited-state reduction potentials ($Ru^{III}L_3/Ru^{II}L_3$*) for c-RuL_3[16] and p-RuL_3[20] are −0.68 and −0.46 V (vs NHE), respectively.

$$Ru^{II}L_3{}^*-TiO_2 \rightarrow Ru^{III}L_3-TiO_2 + e_{cb}^- \quad (1)$$

$$CCl_4 + e_{cb}^- \rightarrow {}^\bullet CCl_3 + Cl^- \quad (2)$$

$$CCl_3CO_2^- + e_{cb}^- \rightarrow {}^\bullet CCl_2CO_2^- + Cl^- \quad (3)$$

The photogenerated chloride concentration greatly exceeded the initial sensitizer concentration (10 μM), which indicates that the oxidized sensitizers should be regenerated. We recently

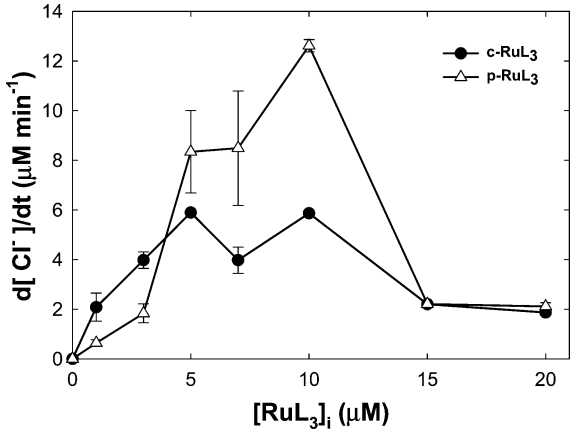

Figure 3. Initial rates of TCA dechlorination under visible light as a function of the ruthenium sensitizer concentration. The experimental conditions were the same as those of Figure 2.

confirmed that water can serve as an electron donor to reduce $Ru^{III}L_3$ to $Ru^{II}L_3$ (reaction 4; step 5 in Scheme 1).[18] The reported

$$2Ru^{III}L_3 + H_2O \rightarrow 2Ru^{II}L_3 + 2H^+ + {}^1/_2O_2 \quad (4)$$

half-wave potentials for the $Ru^{III}L_3/Ru^{II}L_3$ couple for c-RuL_3[16] and p-RuL_3[20] are 1.31 and 1.63 V_{NHE}, respectively, while the standard reduction potential of the O_2/H_2O couple is 1.23 V_{NHE} (1.05 V at pH 3). Although reaction 4 is thermodynamically allowed for both c-RuL_3 and p-RuL_3, the latter has a higher driving force for the regeneration (0.58 vs 0.26 V at pH 3).

Despite the weaker visible light absorption by p-RuL_3 (Figure 1), p-RuL_3 was comparable to (or slightly better than) c-RuL_3 in inducing the dechlorination. This implies that the electron transfer from excited p-RuL_3 to substrates through TiO_2 CB is more efficient than that with c-RuL_3. Since it has been previously reported that phosphonate and phosphinate groups could be strongly coupled onto a TiO_2 surface after hydrothermal treatment,[32,33] aqueous suspensions of $Pt/TiO_2/RuL_3$ were heated at 120 °C for 3 h in an autoclave to investigate the effect of heat treatment on the photoreactivity. Figure 2 also compares the reactivity of the heat-treated sample with that of the nonheated one. $Pt/TiO_2/c\text{-}RuL_3$ samples with and without the heat treatment were little different in their photoreactivity. However, the visible light reactivity of $Pt/TiO_2/p\text{-}RuL_3$ was markedly enhanced after the hydrothermal treatment. This obviously indicates that the hydrothermal treatment induced a stronger coupling between p-RuL_3 and the TiO_2 surface, whereas the linkage between c-RuL_3 and the TiO_2 surface was little affected by the hydrothermal treatment. Therefore, all the rest of our experiments were carried out using the heat-treated $Pt/TiO_2/p\text{-}RuL_3$ and nonheated $Pt/TiO_2/c\text{-}RuL_3$. In Figure 3, the TCA dechlorination rate with sensitized Pt/TiO_2 was investigated as a function of the ruthenium sensitizer concentration. The visible light activity of both $Pt/TiO_2/c\text{-}RuL_3$ and $Pt/TiO_2/p\text{-}RuL_3$ showed a maximum at $[RuL_3]_i \approx 10\ \mu M$. The optimal sensitizer concentration should be a result of competition for surface adsorption sites between the sensitizer (RuL_3) and the substrate (TCA).[17]

pH Effect. The sensitizer adsorption on TiO_2 should be influenced by both the surface charge and the sensitizer's charge. The TiO_2 surface is negatively charged at alkaline pH (i.e., pH > pH_{zpc}) and positively charged at acidic pH (i.e., pH < pH_{zpc}). The pH_{zpc} value of P25 TiO_2 is known to be 6.25.[7] c-RuL_3 and p-RuL_3 have six and four dissociable protons, respectively. The molecular charge of the fully protonated sensitizer is positive

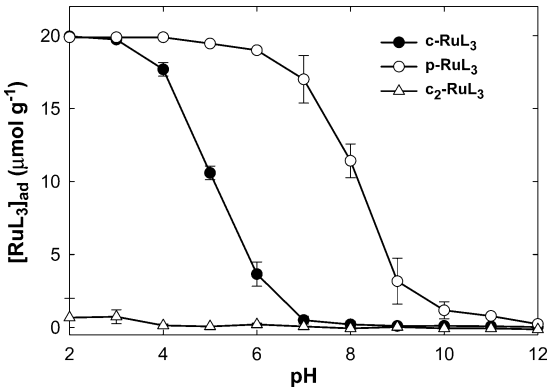

Figure 4. pH-dependent adsorption of c-RuL_3 and p-RuL_3 on TiO_2 under the conditions $[TiO_2] = 0.5$ g/L and $[RuL_3]_i = 10$ μM. As a comparison, it is shown that the adsorption of c_2-RuL_3, which has only two carboxylate groups, is negligibly small.

(+2 at low pH) but gradually changes to negative with increasing pH (−4 for the fully deprotonated c-RuL_3 and −2 for the fully deprotonated p-RuL_3). The complete deprotonation of c-RuL_3 is attained at pH >3,[16] whereas that of p-RuL_3 is expected at pH >12.[21] Therefore, c-RuL_3 carries more negative charge than p-RuL_3. At higher pH, where both the TiO_2 surface charge and the sensitizer's molecular charge are negative, the adsorption of the sensitizer should be negligible (see Figure 4). At pH <6, where the surface charge is positive, c-RuL_3 should be more adsorbed on TiO_2 than p-RuL_3, which carries less negative charge, considering the electrostatic interaction only. However, the pH-dependent adsorption shown in Figure 4 is contrary to the expectation: c-RuL_3 is less adsorbed than p-RuL_3 in the range of pH 3−11. This indicates that the chemical bond formation between the phosphonic acid ($-PO_3H_2$) and the TiO_2 surface hydroxyl group (≡Ti−OH) is highly favored over the ester linkage (≡Ti−OCO−R) formation. In this respect, the phosphonic acid group is more suitable as a stable linkage to TiO_2 surface.

On the other hand, it is very interesting to note that the adsorption of c_2-RuL_3 on a TiO_2 surface was negligibly small in the entire pH region, whereas c-RuL_3 was completely adsorbed at acidic pH. Since only one or two carboxylic groups should be used simultaneously in anchoring c-RuL_3 onto the TiO_2 surface with the other carboxylic groups unbound, such a drastic difference in adsorption between c_2-RuL_3 and c-RuL_3 was hardly expected. The surface binding constant of c_2-RuL_3 on TiO_2, which was measured in *methanol*, is 2×10^4 M^{-1},[22] which indicates that c_2-RuL_3 does adsorb on TiO_2 in methanol solution. The sensitizer adsorption on TiO_2 in aqueous solution should be different from that in methanol. First of all, the charges of c_2-RuL_3, c-RuL_3, and TiO_2 surface are different from those in organic solvent, which should affect the sensitizer adsorption. Another possibility is that c-RuL_3 in water preferably adsorbs onto the TiO_2 surface using two carboxylic groups from neighboring bipyridyl ligands, not from the same bipyridyl ligand. In this case, c_2-RuL_3 cannot satisfy the requirement for efficient adsorption. Further work is required to address this issue.

Figure 5 compares the pH dependence of the CCl_4 (Figure 5a) and TCA (Figure 5b) dechlorination rates between Pt/TiO_2/c-RuL_3 and Pt/TiO_2/p-RuL_3 systems. Since the excited sensitizer should be adsorbed on TiO_2 to transfer an electron to CB, the pH-dependent photoreactivities were qualitatively similar to the pH-dependent adsorption shown in Figure 4. The photoreactivities of Pt/TiO_2/p-RuL_3 were consistently higher than those of Pt/TiO_2/c-RuL_3 over the whole pH range. That is, p-RuL_3 is more strongly attached onto the TiO_2 surface and hence induces higher photoreactivities.

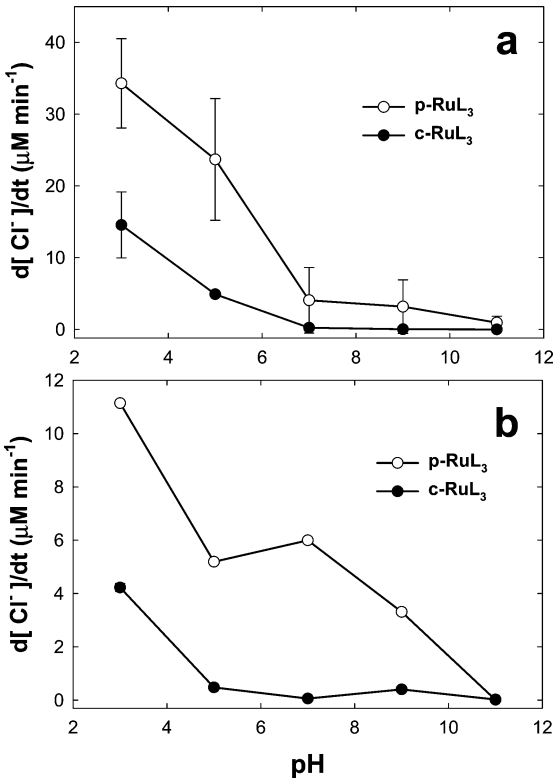

Figure 5. pH-dependent dechlorination rates of (a) CCl_4 and (b) TCA on Pt/TiO_2/c-RuL_3 and Pt/TiO_2/p-RuL_3 under visible light.

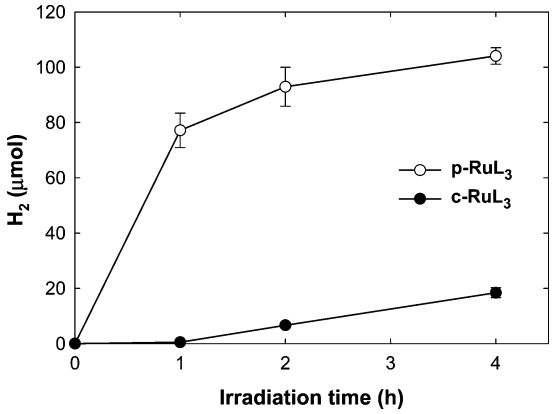

Figure 6. Hydrogen evolution in a visible-light-irradiated Pt/TiO_2/RuL_3 suspension. The experimental conditions were as follows: $[TiO_2] = 0.5$ g/L, $pH_i = 3$, $[RuL_3]_i = 10$ μM, [EDTA] = 10 mM, λ >420 nm, and initially N_2-saturated.

Visible-Light-Induced Hydrogen Production. The visible light reactivity of Pt/TiO_2/RuL_3 was also measured for the hydrogen production (reaction 5).

$$2H^+ + 2e_{cb}^- \rightarrow H_2(g) \qquad (5)$$

The hydrogen generation experiments were carried out under the same conditions of the dechlorination, except for the presence of EDTA as an electron donor. Figure 6 compares the H_2 production under visible light between p-RuL_3- and c-RuL_3-sensitized systems. Pt/TiO_2/p-RuL_3 is far more active than Pt/TiO_2/c-RuL_3 for hydrogen production. This reconfirms that p-RuL_3 anchored on TiO_2 is a more efficient visible light sensitizer than c-RuL_3.

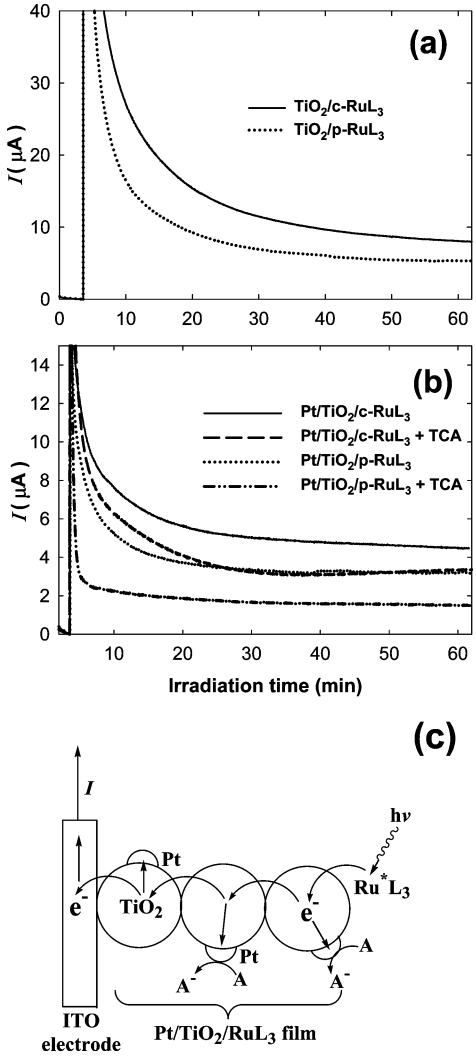

Figure 7. Visible-light-induced photocurrent generation profiles obtained with ITO electrodes coated with (a) TiO_2/RuL_3 and (b) $Pt/TiO_2/RuL_3$ (applied voltage 0.5 V vs SCE) in aqueous electrolytes (pH 3). Photocurrent profiles generated in the absence or presence of TCA are compared. (c) Schematic illustration of the electron-transfer paths on the visible-light-illuminated $Pt/TiO_2/RuL_3$ electrode (A represents electron acceptors such as TCA).

Photocurrent Measurements. Since c-RuL_3 has a higher visible light absorptivity than p-RuL_3 (see Figure 1) and the electron injection (step 1 in Scheme 1) proceeds very rapidly with near 100% efficiency,[13] the number of electrons injected into TiO_2 CB should be larger in $Pt/TiO_2/c\text{-}RuL_3$ than in $Pt/TiO_2/p\text{-}RuL_3$, provided that the same number of sensitizers are adsorbed on TiO_2. Figure 4 indeed shows that the adsorbed concentrations of c-RuL_3 and p-RuL_3 are the same at pH 3. Nevertheless, the photoreactivities were higher with the p-RuL_3 sensitizer for both the dechlorination and hydrogen production. To investigate the effect of different sensitizers on the photoinduced electron-transfer behavior, photocurrent generation profiles obtained with sensitized TiO_2 electrodes under visible light are compared in Figure 7 ((a) $TiO_2/c\text{-}RuL_3$ vs $TiO_2/p\text{-}RuL_3$; (b) $Pt/TiO_2/c\text{-}RuL_3$ vs $Pt/TiO_2/p\text{-}RuL_3$). The scheme in Figure 7c illustrates primary electron-transfer paths in the illuminated $Pt/TiO_2/RuL_3$ electrode. In both part a and part b of Figure 7, the electrodes sensitized by c-RuL_3 exhibit higher photocurrents at the steady state, which is consistent with the higher visible light absorption by c-RuL_3. That is, c-RuL_3 absorbs more visible light photons, injects more electrons, hence induces higher photocurrents but lower photoreactivities, in contrast with expectation. The apparent photonic efficiency of the current generation at the steady state was estimated to be about 3×10^{-5} with the $TiO_2/c\text{-}RuL_3$ electrode. The only plausible explanation for this is the difference in either the recombination rate (step 2 in Scheme 1) or the sensitizer regeneration rate (step 5 in Scheme 1) between $Pt/TiO_2/c\text{-}RuL_3$ and $Pt/TiO_2/p\text{-}RuL_3$ systems, since the electron injection rate (step 1 in Scheme 1) is sufficiently fast regardless of the kind of Ru complex,[13,22] and the kinetics of electron trapping in Pt (step 3 in Scheme 1) should be the same between the two systems. The recombination rate changes the overall photoreactivity, and the fact that the codeposition of Pt on RuL_3/TiO_2 greatly enhances the visible light reactivity has been ascribed to the competition between the electron trapping in Pt and the recombination.[18] However, it is unlikely that the kind of anchoring group in the ruthenium sensitizer influences the recombination rate significantly, because the recombination of the electrons with the oxidized Ru complex involves a d orbital localized on the Ru metal, not ligand orbitals.[13] The thermodynamic driving force for the recombination is sufficiently high (>1.5 V) for both sensitizers. Therefore, the difference in the sensitizer regeneration rate seems to be important. Since p-RuL_3 has a higher driving force for the regeneration reaction than c-RuL_3 (0.58 vs 0.26 V, as has been discussed), the oxidized p-RuL_3 should be more rapidly regenerated. Since the photogenerated chloride concentration exceeds the sensitizer concentration by more than 100-fold (see Figure 2), the sensitizer regeneration step is critical in determining the overall photoreactivity. This may explain the higher photoreactivity of the $Pt/TiO_2/p\text{-}RuL_3$ system. Incidentally, it should be kept in mind that the electron-transfer kinetics in a suspended particle is different from that in a thin film electrode. TiO_2 particles in the thin film are interconnected (as shown in Figure 7c) and injected electrons rapidly migrate from particle to particle to reach the ITO electrode, which is well-known from the studies of dye-sensitized TiO_2 solar cells.[13] It should be also noted that the photocurrents are lower in the presence of Pt deposits (Figure 7a vs Figure 7b) and even lower in the presence of TCA (electron acceptor) (Figure 7b). This is in accord with what the scheme in Figure 7c illustrates: as more electrons are intercepted by a trapping in Pt or an interfacial transfer to TCA, fewer electrons reach the ITO electrode to generate lower photocurrents.

Stability of Anchored Sensitizers in Water and FT-IR Analysis. It is known that c-RuL_3 attached to a TiO_2 surface via an ester linkage is not stable toward hydrolysis.[19−22] The sensitizers might be degraded under visible light irradiation. The stability of ester and phosphonate linkages was compared by measuring photoreactivities of the sensitized photocatalysts as a function of the preirradiation time. Figure 8 shows the effect of the preirradiation time on the initial dechlorination rates of CCl_4 and TCA with $Pt/TiO_2/c\text{-}RuL_3$ or $Pt/TiO_2/p\text{-}RuL_3$. Both photocatalysts gradually lost activity with an increase in preirradiation time, although the reactivity of $Pt/TiO_2/p\text{-}RuL_3$ was consistently higher than that of $Pt/TiO_2/c\text{-}RuL_3$. $Pt/TiO_2/RuL_3$ suspensions stirred for 24 h in the dark also exhibited a significant reduction in the visible light reactivity. The phosphonate linkage as well as the ester linkage to the TiO_2 surface seems to be unstable in water even in the dark.

To check out the possibility of the sensitizer degradation on TiO_2 under visible light, the UV−visible absorption spectra of RuL_3 before and after photoirradiation are compared in Figure 9. Adsorbed sensitizers could be quantitatively recovered from the TiO_2 surface by desorbing them at alkaline pH and filtering

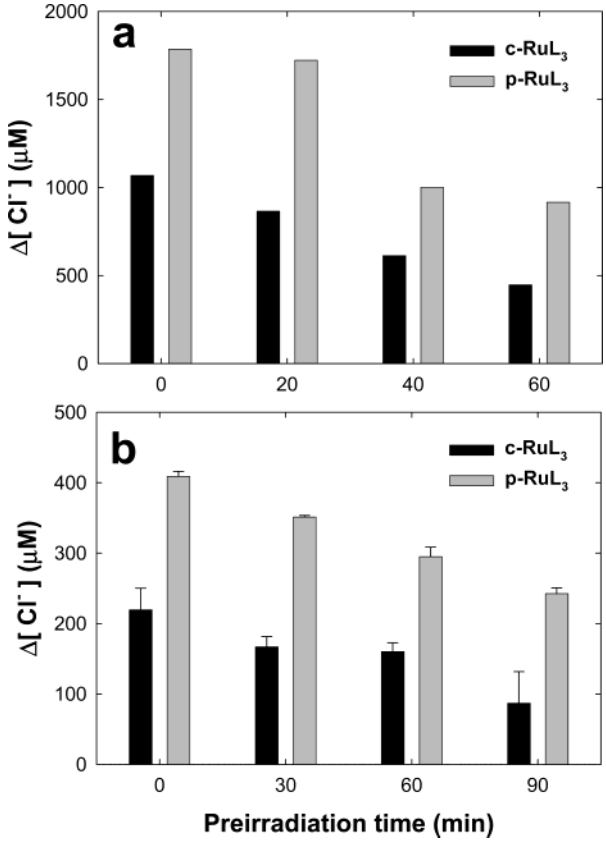

Figure 8. Effects of preirradiation (visible light) time on the initial dechlorination rates of (a) CCl_4 and (b) TCA on $Pt/TiO_2/c\text{-}RuL_3$ and $Pt/TiO_2/p\text{-}RuL_3$ under visible light. Other experimental conditions were the same as those of Figure 2.

out TiO_2 particles. After 6 h of visible light irradiation of $Pt/TiO_2/RuL_3$ suspensions, the intensities of the sensitizer absorption bands are reduced in the region of both ligand excitation ($\pi \rightarrow \pi^*$) and MLCT ($d \rightarrow \pi^*$), which indicates that the sensitizers were degraded. The ruthenium sensitizers recovered from the $Pt/TiO_2/RuL_3$ suspension stirred in the dark for 12 h did not show any sign of reduction in the absorption intensities. Homogeneous RuL_3 solution (without Pt/TiO_2) showed no change in the absorption spectrum after 6 h visible light irradiation (spectrum not shown). This indicates that the visible-light-induced degradation of RuL_3 takes place only when it is attached on TiO_2 and that the efficiency of the sensitizer regeneration (step 5 in Scheme 1 or reaction 4) is not sufficient enough to prevent the sensitizer degradation completely. When 2-propanol (1 mM) was added as an electron donor, the sensitizer degradation could be reduced but not completely prohibited, either.

To investigate how the anchored ruthenium sensitizer changes in water with time, the DRIFT spectra of $c\text{-}RuL_3/TiO_2$ and $p\text{-}RuL_3/TiO_2$ before and after the 24 h hydrolysis were obtained. Different binding structures of the sensitizer anchored on a TiO_2 surface should be reflected in the IR spectra. The possible bonding modes are mono- and bidentate for the $c\text{-}RuL_3$ sensitizer[34] and mono-, bi-, and tridentate for the $p\text{-}RuL_3$ sensitizer,[32] as illustrated in Chart 1.

The DRIFT spectra (1100−1800 cm^{-1} region) of $c\text{-}RuL_3$ adsorbed on TiO_2 ($c\text{-}RuL_3/TiO_2$) and free $c\text{-}RuL_3$ are compared in Figure 10a. Major IR bands of free $c\text{-}RuL_3$ are as follows: 1728 cm^{-1} for the C═O stretching mode; 1612 cm^{-1} for the antisymmetric stretching of $-CO_2^-$; 1367 cm^{-1} for the symmetric stretching of $-CO_2^-$; 1143 cm^{-1} for C−O−H bending;

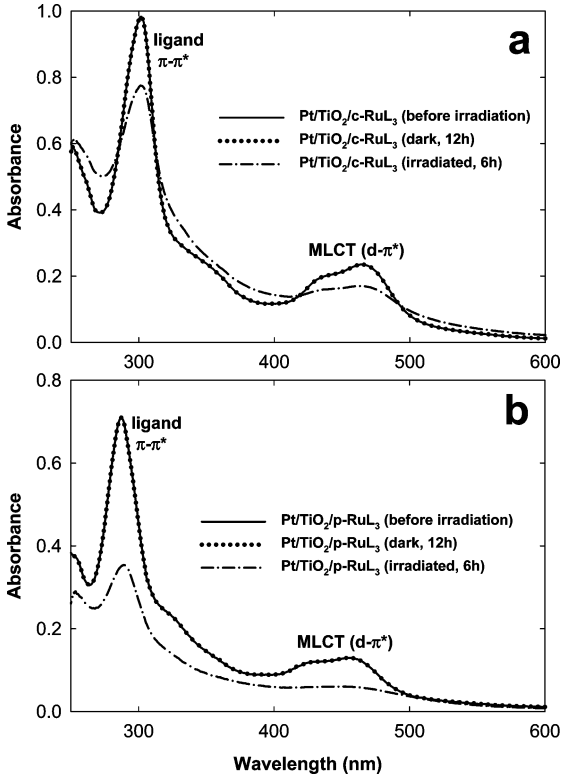

Figure 9. UV−vis absorption spectral changes of (a) $c\text{-}RuL_3$ and (b) $p\text{-}RuL_3$ (desorbed from $Pt/TiO_2/RuL_3$) before and after visible light irradiation (6 h). The dark control spectra are shown together. The experimental conditions were the same as those of Figure 2.

CHART 1: Structures of the Possible Surface Complexes of (a) $c\text{-}RuL_3$ and (b) $p\text{-}RuL_3$ Anchored on TiO_2

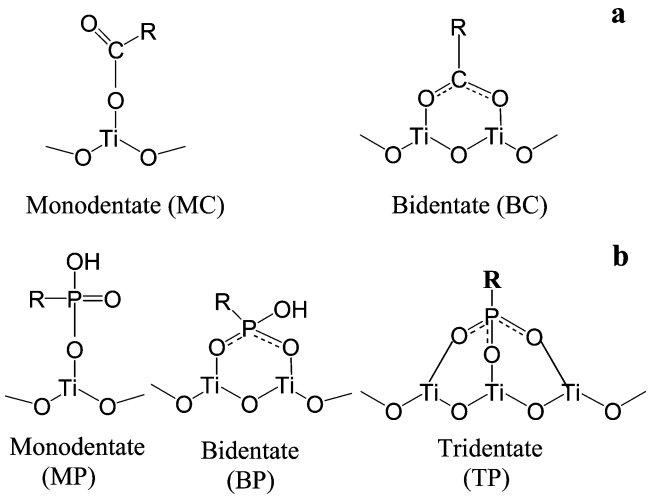

1234 cm^{-1} for singly bonded C−O stretching; 1406, 1431, 1462, and 1550 cm^{-1} for bipyridyl ligand vibration modes.[34−37] The fact that both C═O and $-CO_2^-$ stretching bands were observed indicates that both protonated and deprotonated carboxylic groups are present in the free $c\text{-}RuL_3$ sample. The IR spectrum of $c\text{-}RuL_3$ adsorbed on TiO_2 was little changed in the 1300−1700 cm^{-1} region. The most prominent change is the band at 1726 cm^{-1} (ν(C═O)), whose intensity was greatly reduced on TiO_2. This indicates that the surface complexes of $c\text{-}RuL_3$ are attached through a bidentate coordination (BC), not a monodentate coordination (MC) (see Chart 1a). The band at 1143 cm^{-1} (δ(C−O−H)) was also absent upon adsorbing on TiO_2, which reconfirms the bidentate surface complex formation. Since

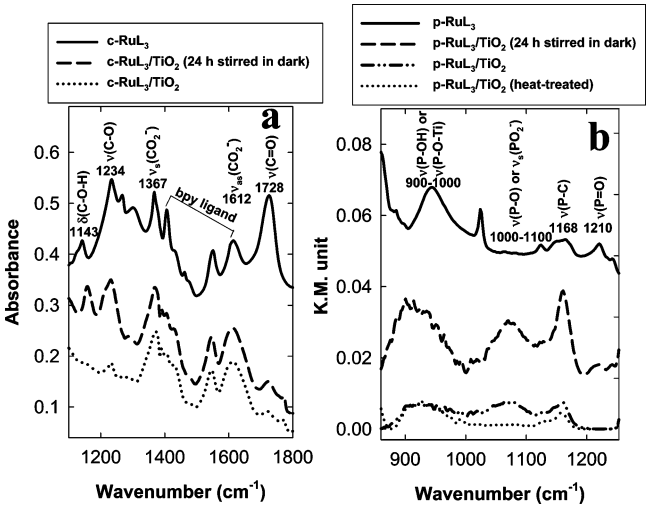

Figure 10. Diffuse-reflectance FT-IR spectra of (a) TiO_2/c-RuL_3 (diluted KBr, referenced against KBr) and (b) TiO_2/p-RuL_3 (referenced against TiO_2) powder samples. The spectrum of free p-RuL_3 was obtained in a transmission mode with a ZnSe window (sample cast), and its IR absorption intensities are relative (not in K. M. unit).

not all six carboxylate groups are bonded to the TiO_2 surface, the ν(C═O) band contributed by the nonbonded acid groups should remain unchanged even after the adsorption on TiO_2. Therefore, the fact that the ν(C═O) band intensity drastically decreased also indicates that the fraction of protonated carboxylate groups (−COOH) in c-RuL_3 significantly decreased during the preparation of the c-RuL_3/TiO_2 sample. On the other hand, the IR spectrum of the TiO_2/c-RuL_3 sample that was stirred for 24 h in the dark as an aqueous suspension and then dried shows the appearance of bands at 1160 and 1230 cm^{-1}. They are characteristic of singly bonded C−O stretching modes with some admixture of C−O−H bending. The C═O stretching band intensity at 1726 cm^{-1} also increased twice. This spectral change implies that the protonated carboxylic groups in the adsorbed sensitizer increased as a result of the hydrolytic cleavage and the subsequent protonation of the anchoring group.[34,35] The gradual loss of photoreactivity of c-RuL_3/TiO_2 with time seems to be related to this structural change in the anchoring group as well as the photosensitized degradation of c-RuL_3 on TiO_2.

Figure 10b compares the IR spectra (860−1250 cm^{-1} region) of the p-RuL_3 adsorbed on TiO_2 and free p-RuL_3. The assignments of some IR bands are as follows: 1210 cm^{-1} to the P═O stretching mode;[32] 1168 cm^{-1} to the P−C stretching mode;[32] 1000−1100 cm^{-1} to the predominantly uncomplexed O−P−O stretching mode;[39,41] 900−1000 cm^{-1} to the P−OH or P−O−Ti stretching mode (it is difficult to distinguish them).[33,41] As for p-RuL_3/TiO_2, the disappearance of the P═O stretching band near 1210 cm^{-1} and the bands at 900−1000 cm^{-1} (the region of P−OH or P−O−Ti stretching modes) suggest the presence of a bidentate (BP) or tridentate (TP) coordination complex (Chart 1b).[32,38−41] The absorption band between 1000 and 1100 cm^{-1} indicates the presence of uncomplexed O−P−O (or PO_2^-) groups on TiO_2, but this band disappeared after the heat treatment. This indicates that the heat treatment induced a stronger surface complexation of p-RuL_3 on TiO_2 and is consistent with the higher photoreactivity of the heat-treated p-RuL_3/TiO_2. On the other hand, the IR spectrum of the TiO_2/p-RuL_3 sample that was stirred for 24 h in the dark as a suspension and then dried shows the reappearance of the band at 1210 cm^{-1} (P═O stretching mode), which indicates that the bidentate or tridentate surface complex is slowly hydrolyzed in water into a monodentate linkage (MP). The gradual loss of photoreactivity of p-RuL_3/TiO_2 with time should be also ascribed to the hydrolytic cleavage of the phosphonate linkage as well as the photosensitized degradation of p-RuL_3 on TiO_2, as in the case of c-RuL_3/TiO_2.

Conclusions

Developing stable and efficient visible light photocatalysts is a challenging issue. Sensitized TiO_2 has been often studied for this purpose, but the stability in water remains unsatisfactory. The stability in aqueous solution is a critical requirement since two major applications of visible light photocatalysts that are water splitting and pollutant degradation should be carried out in water. In this study, we compared the reactivity and stability of two sensitized TiO_2 photocatalysts (Pt/TiO_2/c-RuL_3 vs Pt/TiO_2/p-RuL_3) in water. Although it was expected that the phosphonate linkage to the TiO_2 surface could be more stable than the carboxylate linkage, both turned out to be unstable in water not only under visible light illumination but also in the dark. Ruthenium complexes anchored on TiO_2 were gradually photodegraded under visible light, and the linkage groups were slowly hydrolyzed in the absence of light. Nevertheless, Pt/TiO_2/p-RuL_3 exhibited consistently higher visible light reactivities in water than Pt/TiO_2/c-RuL_3 for all tested reactions and conditions, despite the fact that p-RuL_3 has a lower visible light absorptivity than c-RuL_3. Though not stable enough, the phosphonate group seems to be better than the carboxylate group as a ruthenium sensitizer linkage to the TiO_2 surface in aqueous environments.

Acknowledgment. This work was supported by the Hydrogen Energy R&D Center (21st Century Frontier R&D Program, MOST), by KOSEF through the Center for Integrated Molecular Systems (CIMS), and partially by the Brain Korea 21 project.

References and Notes

(1) Khan, S. V. M.; Al-Shahry, M.; Ingler, W. B., Jr. *Science* **2002**, *297*, 2243.

(2) Abe, R.; Hara, K.; Sayama, K.; Domen, K.; Arakawa, H. *J. Photochem. Photobiol. A: Chem.* **2000**, *137*, 63.

(3) Kim, H. G.; Hwang, D. W.; Kim, J.; Kim, Y. G.; Lee, J. S. *Chem. Commun.* **1999**, 1077.

(4) Yoneyama, H. *Catal. Today* **1997**, *39*, 169.

(5) Kaneco, S.; Shimizu, Y.; Ohta, K.; Mizuno, T. *J. Photochem. Photobiol. A: Chem.* **1998**, *115*, 223.

(6) Xie, T. F.; Wang, D. J.; Zhu, L. J.; Li, T. J.; Xu, Y. J. *Mater. Chem. Phys.* **2001**, *70*, 103.

(7) Hoffmann, M. R.; Martin, S. T.; Choi, W.; Bahnemann, D. W. *Chem. Rev.* **1995**, *95*, 69.

(8) *Photocatalytic Purification and Treatment of Water and Air*; Ollis, D. F., Al-Ekabi, H., Eds.; Elsevier: Amsterdam, 1993.

(9) (a) Choi, W.; Hong, S. J.; Chang, Y.-S.; Cho, Y. *Environ. Sci. Technol.* **2000**, *34*, 4810. (b) Choi, W.; Ko, J. Y.; Park, H.; Chung, J. S. *Appl. Catal. B: Environ.* **2001**, *31*, 209. (c) Kim, S.; Choi, W. *Environ. Sci. Technol.* **2002**, *36*, 2019. (d) Lee, J.; Park, H.; Choi, W. *Environ. Sci. Technol.* **2002**, *36*, 5462. (e) Lee, M. C.; Choi, W. *J. Phys. Chem. B* **2002**, *106*, 11818. (f) Vohra, M. S.; Kim, S.; Choi, W. *J. Photochem. Photobiol. A: Chem.* **2003**, *160*, 55. (g) Hwang, S.; Lee, M. C.; Choi, W. *Appl. Catal. B: Environ.* **2003**, *46*, 49. (h) Choi, W.; Lee. J.; Kim, S.; Hwang, S.; Lee, M. C.; Lee, T. K. *J. Ind. Eng. Chem.* **2003**, *9*, 96.

(10) Choi, W.; Termin, A.; Hoffmann, M. R. *J. Phys. Chem.* **1994**, *98*, 13669.

(11) Asahi, R.; Morikawa, T.; Ohwaki, T.; Aoki, K.; Taga, Y. *Science* **2001**, *293*, 269.

(12) O'Regan, B.; Grätzel, M. *Nature* **1991**, *353*, 737.

(13) Hagfeldt, A.; Grätzel, M. *Chem. Rev.* **1995**, *95*, 49.

(14) Fessenden, R. W.; Kamat, P. V. *J. Phys. Chem.* **1995**, *99*, 12902.

(15) Stipkala, J. M.; Castellano, F. N.; Heimer, T. A.; Kelly, C. A.; Livi, K. J. T.; Meyer, G. J. *Chem. Mater.* **1997**, *9*, 2341.

(16) Lobedank, J.; Bellmann, E.; Bendig, J. *J. Photochem. Photobiol. A: Chem.* **1997**, *108*, 89.

(17) Cho, Y.; Choi, W.; Lee, C.-H.; Hyeon, T.; Lee, H.-I. *Environ. Sci. Technol.* **2001**, *35*, 966.
(18) Bae, E.; Choi, W. *Environ. Sci. Technol.* **2003**, *37*, 147.
(19) Péchy, P.; Rotzinger, F. P., Nazeeruddin, M. K.; Kohle, O.; Zakeeruddin, S. M.; Humphry-Baker, R.; Grätzel, M. *J. Chem. Soc., Chem. Commun*. **1995**, 65.
(20) Trammell, S. A.; Moss, J. A.; Yang, J. C.; Nakhle, B. M.; Slate, C. A.; Odobel, F.; Sykora, M.; Erickson, B. W.; Meyer, T. J. *Inorg. Chem*. **1999**, *38*, 3665.
(21) Montalti, M.; Wadhwa, S.; Kim, W. Y.; Kipp, R. A.; Schmehl, R. H. *Inorg. Chem*. **2000**, *39*, 76.
(22) Gillaizeau-Gauthier, I.; Odobel, F.; Alebbi, M.; Argazzi, R.; Costa, E.; Bignozzi, C. A.; Qu, P.; Meyer, G. J. *Inorg. Chem*. **2001**, *40*, 6073.
(23) Merrins, A.; Kleverlaan, C.; Will, G.; Rao, S. N.; Scandola, F.; Fitzmaurice, D. *J. Phys. Chem. B* **2001**, *105*, 2998.
(24) Qu, P.; Meyer, G. J. *Langmuir* **2001**, *17*, 6720.
(25) Haginiwa, J. *J. Pharm. Soc. Jpn*. **1955**, *75*, 731.
(26) Wenkert, D.; Woodward, R. B. *J. Org. Chem*. **1983**, *48*, 283.
(27) Maerker, G.; Case, F. H. *J. Am. Chem. Soc*. **1958**, *80*, 2745.
(28) Penicaud, V.; Odobel, F.; Bujoli, B. *Teteahedron Lett.* **1998**, *39*, 3689.
(29) Vlachopoulos, N.; Liska, P.; Augustynski, J.; Grätzel, M. *J. Am. Chem. Soc*. **1988**, *110*, 1216.
(30) Park, H.; Kim, K. Y.; Choi, W. *J. Phys. Chem. B* **2002**, *106*, 4775.
(31) Heller, H. G.; Langan, J. R. *J. Chem. Soc., Perkin Trans. 2* **1981**, 341.
(32) Guerrero, G.; Mutin, P. H.; Vioux. A. *Chem. Mater*. **2001**, *13*, 4367.
(33) Gawalt, E. S.; Avaltroni, M. J.; Koch, N.; Schwartz, J. *Langmuir* **2001**, *17*, 5736.
(34) Finnie, K. S.; Bartlett, J. R.; Woolfrey, J. L. *Langmuir* **1998**, *14*, 2744.
(35) Roddick-Lanzilotta, A. D.; McQuillan, A. J. *J. Colloid Interface Sci*. **1999**, *217*, 194.
(36) Qu, P.; Thompson, D. W.; Meyer, G. J. *Langmuir* **2000**, *16*, 4662.
(37) Nazeeruddin, M. K.; Amirnasr, M.; Comte, P.; Mackay, J. R.; McQuillan, A. J.; Houriet, R.; Grätzel, M. *Langmuir* **2000**, *16*, 8525.
(38) Socrates, G. *Infrared Characteristic Group Frequencies*, 2nd ed.; Wiley: New York, 1994.
(39) Rusu, C. N.; Yates, J. T., Jr. *J. Phys. Chem. B* **2000**, *104*, 12292.
(40) Barańska, M.; Chruszcz, K.; Małek, K.; Kulinowska, J.; Proniewicz, L. M. *Vib. Spectrosc*. **2003**, *33*, 83.
(41) Sheals, J.; Sjöberg, S.; Persson, P. *Environ. Sci. Technol.* **2002**, *36*, 3090.